Electron-Ion Collision Studies Using a 14.0 GHz ECRIS

Ara Chutjian, Jason B. Greenwood and Steven J. Smith

Atomic and Molecular Collisions Team
Jet Propulsion Laboratory, California Institute of Technology, Pasadena, CA 91109

A new 14.0 GHz electron-cyclotron resonance ion source, the so-called *Caprice* source, has been in operation at JPL/Caltech for over a year. The source produces ample currents of multiply-charged ions (MCIs) for atomic-physics measurements, in particular of MCIs that are of astrophysical interest. Studies at JPL are carried out using *Caprice* and a three-way beam switcher allowing one to make measurements of absolute electron-ion excitation cross sections using electron energy loss and merged or crossed beams, f-values of metastable states using a Kingdon ion trap, and absolute ion-neutral charge exchange cross sections, with X-ray detection, in a beam line presently being tested.

INTRODUCTION

The development of sources for multiply-charged ions (MCIs) has opened up new vistas in several exciting areas of atomic physics. Ions corresponding to plasmas as hot as a fusion reactor, and a solar or stellar atmosphere, can be generated in the laboratory. Measurements can be made of badly-needed plasma parameters, such as cross sections for electron excitation, charge-exchange, X-ray emission, and dielectronic recombination; and *f*-values for allowed (E1) and metastable transitions (E2, E3, M1). When combined with electron energy-loss methods, these measurements can provide new results for the angular distributions of elastic and inelastic electron scattering in MCIs. Such angular distributions provide more rigorous tests of theoretical methods than the angle-averaged integral cross sections.

EXPERIMENTAL TECHNIQUES

The ECR Ion Source

Development of the electron-cyclotron resonance ion source (ECRIS) by Geller and his associates (1) has provided an opportunity for non-storage ring researchers to have within their own space and budget allotments a source of fast MCIs which can be used in experiments. The two popular single-stage versions of the ECRIS are the so-called *Caprice* type, using electromagnets to generate the solenoidal field and permanent magnets for the hexapole field (2), and the *Nanogan* source using permanent magnets throughout (3). A schematic diagram of the *Caprice* ECR source is shown in Fig. 1. Both types use a minimum-B configuration in which energetic electrons are mirrored, and positive ions are confined to suffer (or enjoy) successive ionizations to high charge states, of charge limited by the value of $n_e v_e \tau_i$ (electron density × electron velocity × ion confinement time). Shown in Fig. 2 are the optimum metal-ion currents (electrical) obtained from the Caprice at two operating frequencies. In general, the higher 14.5 GHz frequency affords about a factor of five increase over that obtained at 10 GHz.

Another interesting part comes when such a source is connected to an experimental beams system. Given the astrophysical interests at JPL, the experiments that we have thus far chosen are excitation (using electron

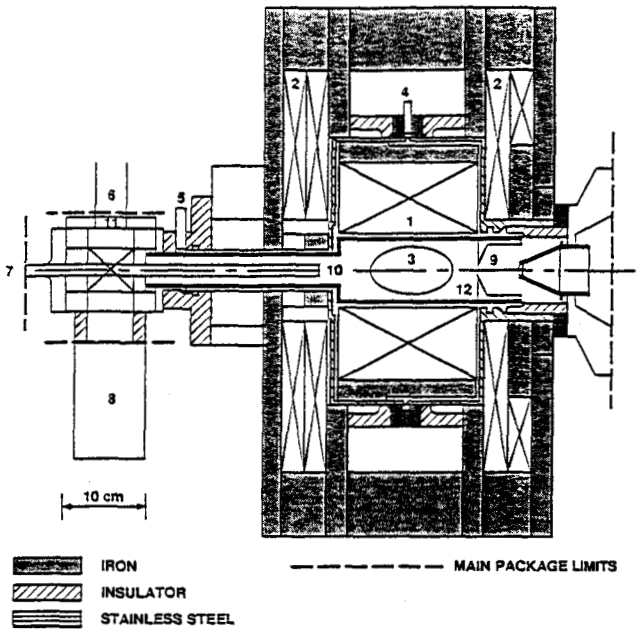

Figure 1. Schematic of the 14 GHz *Caprice* source (from Ref. 1) : (1) hexapole magnets, (2) solenoid coils, (3) closed ECR surface, (4) hexapole magnet water-cooling inlet, (5) water-cooling outlet, (6) microwave power waveguide, (7) coaxial tube gas inlet, (8) 70 *l/s* turbopump, (9) ion extractor, (10) gas outlet, (11) microwave window, (12) removable plasma chamber. The minimum-B configuration gives net magnetic fields of 1.4T-0.4T-1.2T at the left, center, and right of the plasma surface (3).

energy loss), *f*-value measurements (using a Kingdon ion trap), charge-exchange (using retarding-potential difference for ion-state analysis), and X-ray emission (using a thin-window Ge detector). The configuration of the three beam lines is shown in Fig. 3. Further details can be found in Ref. 4.

The Energy-Loss Method

The electron energy-loss method for singly- and multiply-charged ions is a powerful method for obtaining cross sections in spin- and symmetry-forbidden transitions. These transitions are routinely detected in stellar, solar, interstellar, planetary, and cometary absorption and emission spectra. The technique can be described as,

$$(E,0^{\circ}) + A(nl)^{m+} \rightarrow e(E-\Delta E,\theta) + A(n'l')^{m+}$$

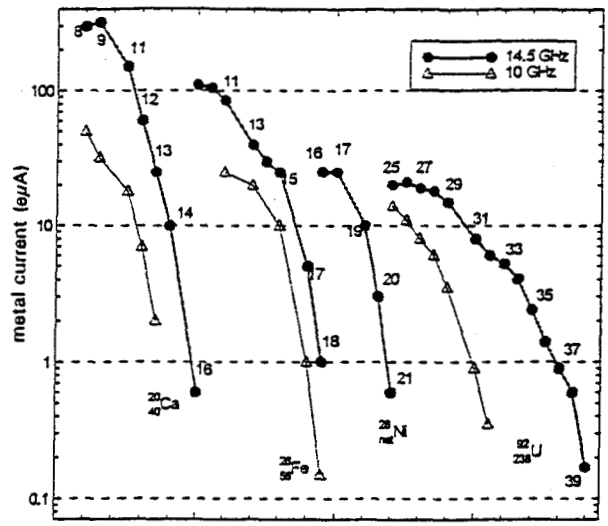

Figure 2. Optimal metal-ion beam currents (electrical) from the *Caprice*, at two operating frequencies (from Ref. 2).

where ΔE is the electron energy loss in the center-of-mass (CM) frame corresponding to the energy difference between the initial *nl* and final *n'l'* states of the ion A^{m+}, and θ is the polar scattering angle. As seen from this equation, one is able to measure *angular distributions* of elastically- and inelastically-scattered electrons. These differential cross sections (DCSs) are not required, at the moment, for astrophysical modeling purposes. They would be needed if, for example, one were interested in mapping the escape trajectories and energies of electrons from within a hot stellar plasma. However, the DCSs *do* provide a more stringent test of theory, since angular results probe both the short-range (large scattering angles, optically-forbidden transitions) and long-range (small scattering angles, optically-allowed transitions) parts of the scattering potential. First measurements using the energy-loss method, in fact, were angular in nature (5). These initial results in e-Zn^{+} scattering are shown in Fig. 4. More recent elastic-scattering DCS in MCIs have been reported by Huber *et al.* (6), and those results are shown for e-Xe^{6+} and e-Xe^{8+} in Fig. 5. Energy-loss results for elastic and

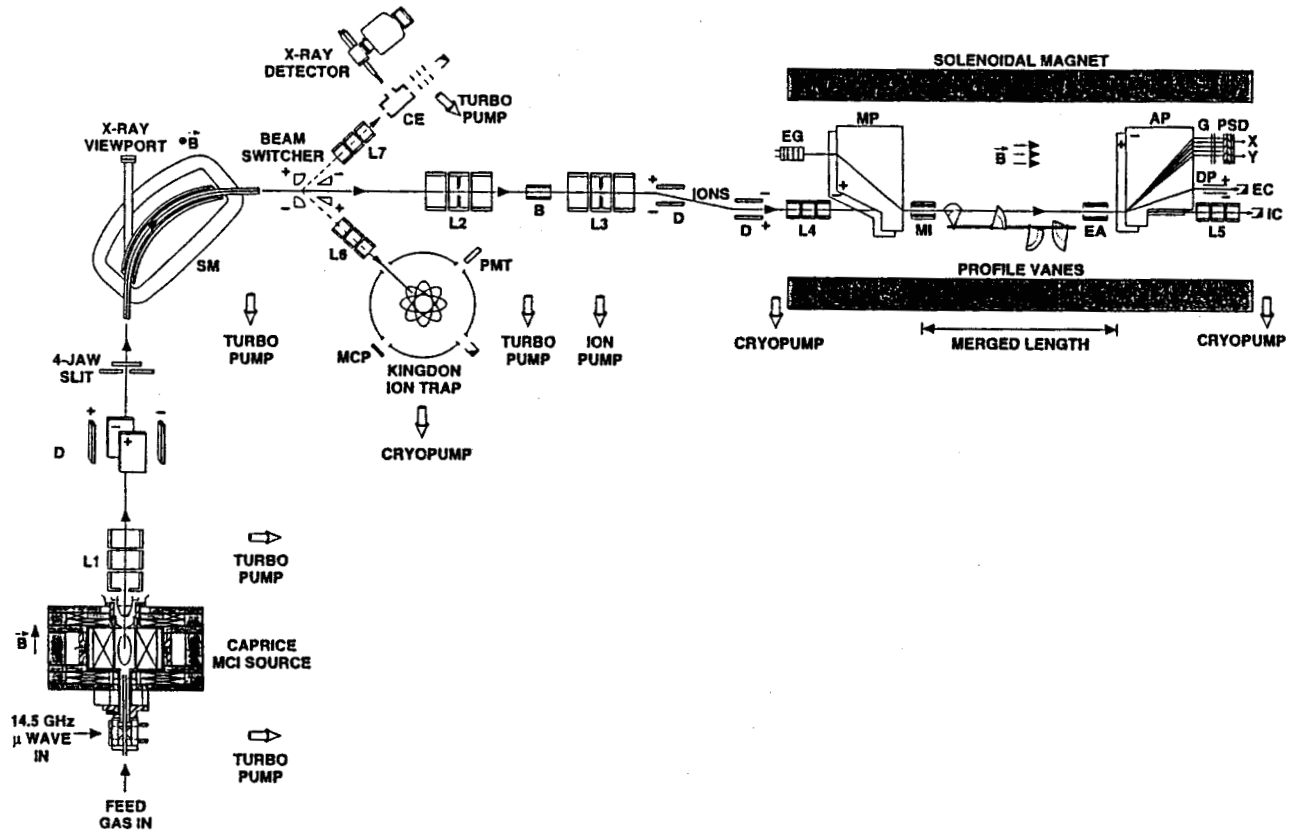

Figure 3. Experimental arrangement of the JPL MCI Facility. (**L1-L7**) three-element electrostatic focusing lenses, (**SM**) mass/charge selection magnet, (**B**) differential pumping baffle, (**D**) deflector plates, (**MP**) merging trochoidal plates, (**AP**) analyzing trochoidal plates, (**MI**) electron mirror, (**EA**) electronic aperture to help discriminate against elastically-scattered electrons, (**DP**) trochoidal plates to deflect parent electron beam out of the scattering plane, (**PSD**) position-sensitive detector, (**G**) electron retarding grids for discrimination, (**EC**) electron Faraday cup, (**IC**) ion Faraday cup, (**CE**) charge-exchange cell, (**MCP**) microchannel plate, (**PMT**) multiplier phototube. The three beam lines after the switcher are for excitation, *f*-value, and charge-exchange/X-ray measurements.

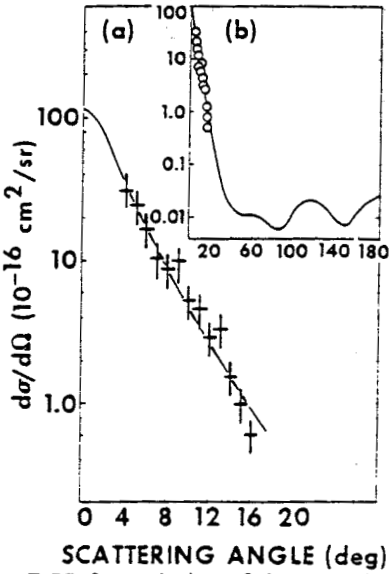

Figure 4. DCS for excitation of the 4s → 4p resonance transition in Zn^+ at E_{CM} = 75 eV, illustrating first use of the energy-loss method in ions. Experiments are crosses, while solid line is the five-state close-coupling calculation, also used to normalize the DCS at $\theta = 14°$ (from Ref. 5).

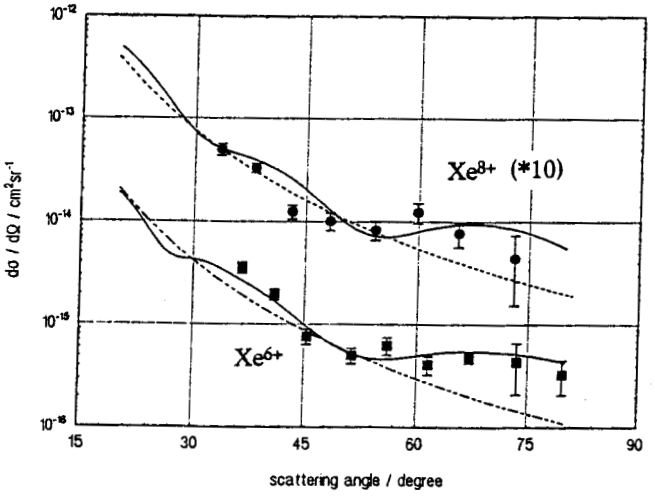

Figure 5. Experimental DCS for elastic scattering at E_{CM} = 50 eV from Xe^{6+} (squares) and Xe^{8+} (filled circles) (from Ref. 6). Theories are Hartree-Fock (solid lines), and Rutherford DCS for C^{6+} and O^{8+} (dashed lines).

superelastic scattering from the Queen's University group are found in Refs. 7 and 8.

Discrimination Against Elastic Scattering

As has been pointed out in previous electron excitation/energy-loss work using merged beams (9,10) the overlap in a trochoidal velocity analyzer between higher-angle elastically-scattered electrons and lower-angle inelastically-scattered electrons can be an important source of interference. Measures must be taken to filter the elastic electrons from the total spectrum. Methods used in the past have been retarding grids (9) (**G** in Fig. 3) and use of fixed-diameter physical apertures (10). There was recently developed at JPL an "electronic aperture" (EA) which uses externally-adjustable electrostatic potentials on an array of poles, to alter the effective cutoff diameter of the electrons spiraling in the solenoidal magnetic field (Fig. 3) (11,12). A schematic diagram of the pole structure is shown in Fig. 6. There are 16 poles, each of 2.00 mm dia and 25 mm long. The axis of the poles is centered on the merged electron-ion beam axis. Equal and opposite potentials are placed on adjacent poles, giving a cancellation of both the electric potential and electric field at the center of the array. Electrons which travel "sufficiently close" to the array axis are at the center of the array. Electrons which therefore undeflected. Electrons having larger Larmor radii (most of the elastic ones!) will make excursions closer to one of the poles, and will spiral into one of the rods, or into the surrounding shield.

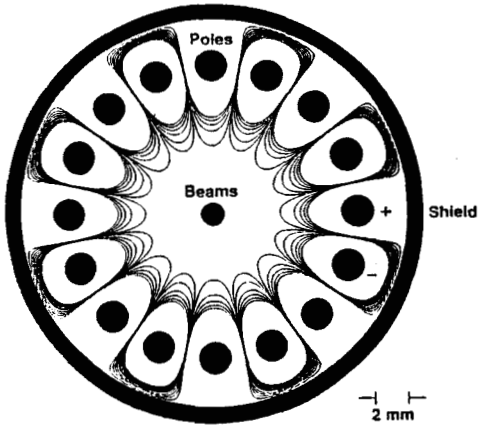

Figure 6. Schematic of the "electronic aperture" (EA) used in MCI excitation measurements. This end-on view shows sixteen rods (dark circles) symmetrically placed about the merged electron and ion beams (shaded central region). Light lines are calculated equipotentials.

In order to understand the orbit discrimination a full three-dimensional field-and-trajectories software code (13) was used to model the trajectories with the precise geometry of the rods, and with the correct applied solenoidal magnetic field and electrostatic rods potentials. Approximately 2000 trajectories at each of four values of the magnetic field were launched, using starting energies and (polar θ, azimuthal ϕ) angles in the CM frame (12). [Many trajectories are also calculated during a merged-beams measurement using the actual experimental voltages.] The effects of the EA can be seen in Fig. 7. One clearly sees the cutoff curves

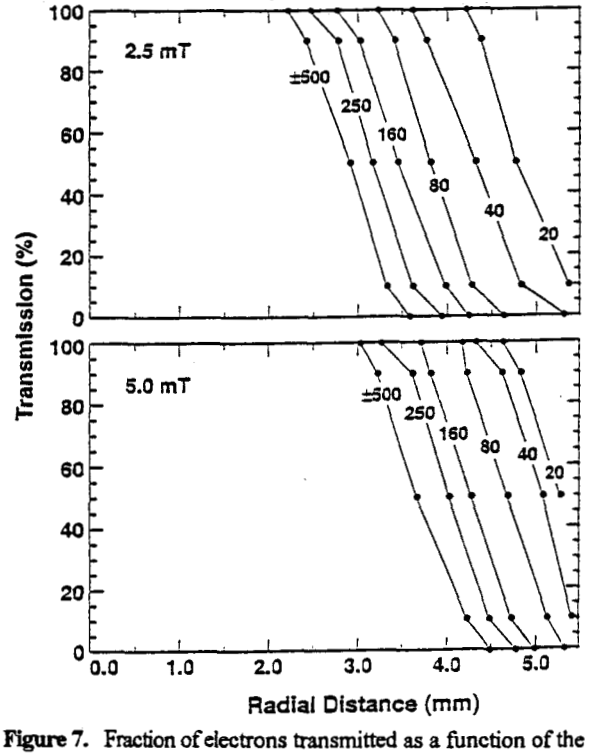

Figure 7. Fraction of electrons transmitted as a function of the maximum excursion of the electrons from the central axis of EA (see Fig. 6), at the indicate solenoidal magnetic fields. The values of the alternating potentials for adjacent rods are indicated on each curve. The 16 poles are centered on a radius of 7.50 mm.

moving towards smaller radial distance (effective aperture size decreasing) as one increases the magnitude of the poles potential. The range of effective diameters of the aperture used herein was 7-12 mm (10% transmission points).

Astrophysical Applications

For the simple case of coronal equilibrium in a hot, dilute plasma one has the expression useful for determining the electron temperature T_e for the excited-state ion population N_i,

$$N_i = N_e N_g C(g \rightarrow i)/A(i \rightarrow g)$$

where g refers to the ionic ground state, and $C(g \rightarrow i)$, $A(i \rightarrow g)$ are the collisonal excitation rate (cm^3/sec) and the spontaneous radiative decay rate (sec^{-1}), respectively. The collision rate is an average of the collision strength or cross section over the (usually) Maxwellian electron energy distribution function of the plasma. This rate includes the effects of resonances near inelastic thresholds. These often sharp, intense resonances are significant contributors to the convoluted excitation rate function. As shown below, the resonances are clearly detected in both experimental and theoretical cross sections.

One of the most fascinating drivers of atomic physics within our solar system is the plasma torus created by exploding volcanoes on Io, a satellite of Jupiter. The SO_2/S_x hurled into the orbit of Io are dissociated and ionized by energetic electrons, ions, and solar UV photons. The ions move and spiral in the Jupiter's inner magnetosphere. This spiraling serves effectively as an ion "bottle," and the O, S particles are successively ionized to higher charge states, up to about O^{3+} and S^{4+} (14). Optical emissions from excited states of these ions in the Io torus are clearly detected in NASA's Voyager, Galileo, and (upcoming) Cassini flybys, by the Hubble Telescope, and by a multitude of high-resolution ground observations.

In order to provide accurate collision strengths to planetary modelers, and to test the theoretical approximations, excitation measurements have been carried out on O^+ (15), S^+ (16) and S^{2+} scattering. Work on the higher O and S charge states is planned. Shown in Figs. 8 and 9 are recent JPL results for S^+ and S^{2+} excitation, respectively, using the energy-loss, merged-beams approach. In each case, there is good agreement of the experimental data with *R*-matrix theory, depending somewhat on the number of states included in the calculation.

Another intriguing and quite unexpected source of atomic physics in our solar system has been the X-ray emissions observed from various comets as they approach the Sun (18,19). The major source of these emissions has been the fully- and partially-stripped solar wind ions (C, N, O, Mg, Ca, *etc.*) streaming from the sun, and charge-exchanging with neutral species boiling off the comet surface. Measurements of these cross sections, as well as the X-ray emission

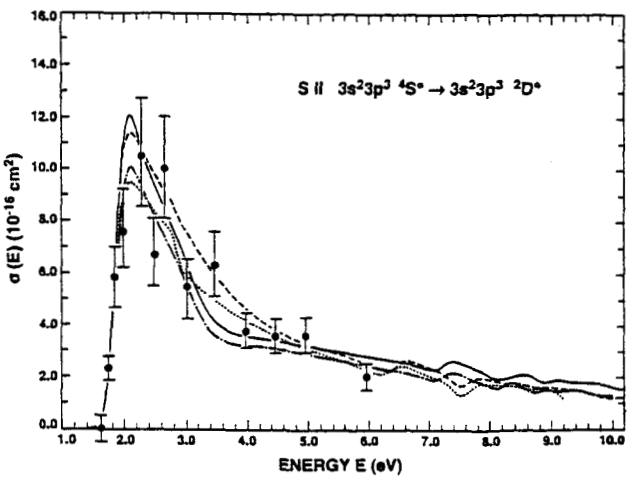

Figure 8. Experimental cross sections *vs* CM energy for excitation of the $^4S^\circ \rightarrow {}^2D^\circ$ transition in S^+ (filled circles). Theories are: 19-state *R*-matrix (solid and dash-dot lines), 12-state *R*-Matrix (dashed line), and 6-state *R*-Matrix (dotted line). See Ref. 16 for details.

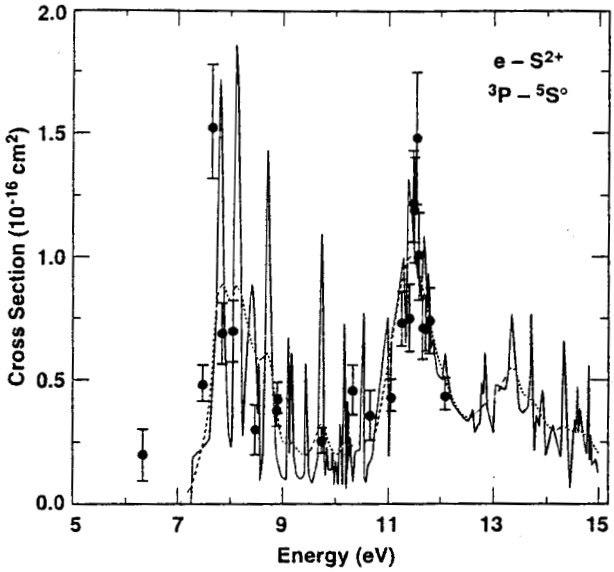

Figure 9. Preliminary experimental (filled circles) and theoretical [solid line (17)] cross sections for the $3s^23p^2\ ^3P \rightarrow 3s3p^3\ ^5S^\circ$ transition in S^{2+}. Dashed line is theory convoluted with a 250 meV FWHM electron-energy resolution.

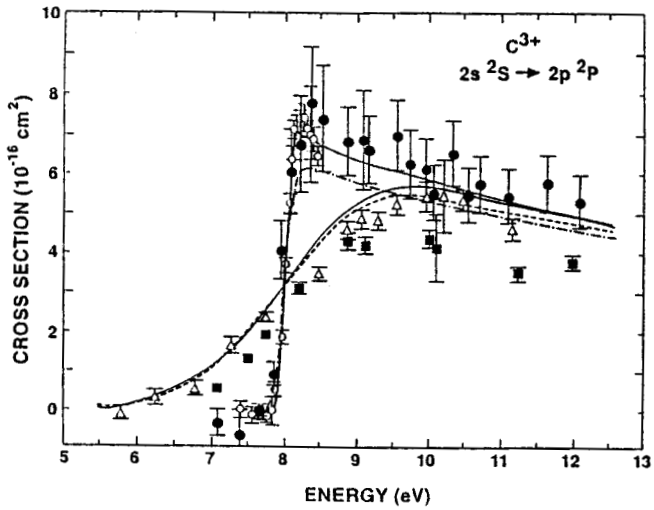

Figure 10. Experimental cross sections for excitation of the 2s $^2S \rightarrow 2p\ ^2P$ transition in C^{3+}. JPL energy-loss data are given as filled circles, and results of Ref. 23 at threshold are shown as open circles. Optical-emission results (folded with a 2.3 eV energy spread) are given as filled squares and open triangles. Theoretical curves are: Coulomb-Born (solid line, folded with a 0.17 eV and 2.3 eV energy spread), two-state close-coupling (dashed line, 2.3 eV energy spread), and nine-state *R*-Matrix (linked line, 0.17 eV energy spread). See Refs. 12 and 23 for further details.

spectra, is proceeding at JPL on the charge-exchange beam line (see Fig. 3).

For the astrophysical objects with higher electron temperature plasmas such as stars, planetary nebulae, and our Sun, rich spectral emissions are detected using NASA's EUVE (20) and HST (21) satellites, and the ESA/NASA SOHO satellite (22). One of the more prominent emitters in these plasmas is the C^{3+} ion. The 2s $^2S \rightarrow 2p\ ^2P$, 1551 Å transition is routinely detected, hence a measure of its collision strength, with comparison to theory, would be critical.

Shown in Fig. 10 are results which combine two experimental results using energy-loss, merged-beams methods (12), (23); and several theoretical calculations. One sees good agreement between the two energy-loss experiments in their overlapping range near threshold. Both the Coulomb-Born and the nine-state *R*-Matrix theories provide a reasonable scattering description for this ubiquitous astrophysical emitter.

SUMMARY

The several excitation examples presented here certainly do not cover the full range of measurements required for modeling any high electron temperature plasma. Needed are data for direct recombination, dielectronic recombination (especially in the presence of magnetic and electric fields), charge exchange, spontaneous transition probabilities, and effective optical emission cross sections (including cascading). Excitation from metastable states of MCIs would again provide a critical test of theory. A stellar atmosphere and the ITER reactor (24) have plasma data needs in common, although the specific target species and charge states may differ.

ACKNOWLEDGMENTS

JBG acknowledges support through the NASA-National Research Council Associateship Program. This work was carried out at JPL/Caltech, and was funded through NASA .

REFERENCES

1. Geller, R., *Rev. Sci. Instr.* **69**, 1302-10 (1998).
2. Hitz, D., Bourg, F., Ludwig, P., Melin, G., Pontonnier, M., and Nguyen, T. K., "The New 1.2T Caprice Source: Presentation and Results," *12th Int. Workshop on ECR Ion Sources*, RIKEN (Japan), April 25-27, 1995.
3. Manoury, L., et al. "NANOGAN II 14.5 GHz: A Compact ECRIS for On Line Production of Multicharged Radioactive Ion Beams for SPIRAL," *Proc. 13th Int. Workshop on ECR Ion Sources*, College Sta. TX, 26-28 Feb. 1997; see also Delaunay, M., *Rev. Sci. Instr.* **61**, 267-9 (1990).
4. Liao, C., Smith, S. J., Chutjian, A., and Hitz, D., *Phys. Scripta* **T73**, 382-3 (1997).
5. Chutjian, A. and Newell, W. R., *Phys. Rev. A* **26**, 2271-3 (1982); Chutjian, A., Msezane, A. Z., and Henry, R. J. W., *Phys. Rev. Letters* **50**, 1357-60 (1983).
6. Huber, B. A., Ristori, C., Guet, C., Küchler, D., and Johnson, W. R., *Phys. Rev. Letters* **73**, 2301-3 (1994).
7. Greenwood, J. B. and Williams, I. D., *Phys. Scripta* **T73**, 108-9 & 121-2 (1997).
8. Srigengan B., Williams, I. D., and Newell, W. R., *J. Phys. B: At. Mol. Phys.* **29**, L605-10 (1996).
9. Smith, S. J. *et al.*, *Phys. Rev. A* **48**, 292-309 (1993).
10. Bell, E. W. *et al.*, *Phys. Rev. A* **49**, 4585-96 (1994).
11. A. Chutjian, J. B. Greenwood, and S. J. Smith, *APS Topical Conf. On Atom. Processes in Plasmas* (in press).
12. J. B. Greenwood, S. J. Smith, and A. Chutjian, *Phys. Rev. A* (in press).
13. D. A. Dahl, SIMION 3D Version 6.0 User's Manual (Idaho Nat. Engin. Lab. Report No. INEL-95/0403
14. Hall, D. T., *et al.*, *Astrophys. J.* **426**, L51-4 (1994); Shemansky, D. E., *J. Geophys. Res.* **93**, 1773-84 (1988).
15. Zuo, M., Smith, S. J., Chutjian, A., Williams, I. D., and Tayal, S. S., *Astrophys. J.* **440**, 421-29 (1995).
16. Liao, C., Smith, S. J., Hitz, D., Chutjian, A., and Tayal, S. S., *Astrophys. J.* **484**, 979-84 (1997).
17. Tayal, S.S., *Astrophys. J.* **481**, 550-6 (1997).
18. Wegmann, R., Schmidt, H. U., Lisse, C. M., Dennerl, K., and Englhauser, J., *Planet. Space Sci.* **47**, 603-12 (1998).
19. Krasnopolsky, V., *J. Geophys. Res.* **103**, 2069-75 (1998).
20. Craig, N., *et al.*, *Astrophys. J. Suppl. Ser.* **113**, 131-93 (1997); Landi. E., Landini, M., and Del Zanna, G., *Astron Astrophys.* **324**, 1027-35 (1997).
21. Vassiliades, E., *et al.*, *Astrophys. J. Suppl. Ser.* **114**, 237-61 (1998).
22. Wilhelm, K., *et al.*, *Astron. Astrophys.* **334**, 685-702 (1998).
23. Bannister, M. E., *et al.*, *Phys. Rev. A* **57**, 278-81 (1998).
24. Horton, L. D., *Phys. Scripta* **T65**, 175-8 (1996).